Electroregulated Metal-Binding with a Crown Ether Tetrathiafulvalene Derivative: Toward Electrochemically Addressed Metal Cation Sponges

Franck Le Derf,[†] Miloud Mazari,[†,⊗] Nicolas Mercier,[†] Eric Levillain,[†] Pascal Richomme,[‡] Jan Becher,[§] Javier Garín,[⊥] Jesus Orduna,[⊥] Alain Gorgues,*[,†] and Marc Sallé*[,†]

Laboratoire d'Ingénierie Moléculaire et Matériaux Organiques, UMR CNRS 6501, Université d'Angers, 2 Bd Lavoisier, F-49045 Angers, France, Laboratoire de Synthèse Organique Appliquée, Université d'Oran Es-Sénia, BP 1524 Oran, Algeria, SC RMN, Université d'Angers, 2 Bd Lavoisier, F-49045 Angers, France, Department of Chemistry, Odense University, Campusvej 55, DK-5230 Odense M, Denmark, and Instituto de Ciencia de Materiales de Aragon, Unidad de Nuevos Materiales Orgánicos Facultad de Ciencias, CSIC-Universidad de Zaragoza, E-50009 Zaragoza, Spain

Received June 30, 1999

A redox responsive ligand incorporating the tetrathiafulvalene unit has been synthesized. The crystal structure of the free ligand (*Z*)-**1** ($C_{20}H_{30}O_5S_8$, triclinic $P\bar{1}$, $Z = 2$, $a = 9.087(6)$ Å, $b = 11.637(7)$ Å, $c = 14.370(8)$ Å, $\alpha = 65.54(3)°$, $\beta = 82.32(5)°$, $\gamma = 84.18(6)°$, $V = 1368$ Å^3) shows the redox-active tetrathiafulvalene core to be essentially planar, which allows observation of two reversible one-electron processes upon electrochemical oxidation. The efficiency of this system in the control of the reversible complexation/expulsion sequence of a metallic cation (i.e., Ba^{2+}) has been made possible thanks to a combination of (a) an unprecedented high coordination ability among tetrathiafulvalene-based macrocycles as determined by LSI mass spectrometry (log $K° = 3.5$, NBA-matrix) as well as by solution investigations (^{1}H NMR and cyclic voltammetry titration studies), which remarkably converge to similar binding constant values (i.e., log $K° = 4.2-4.3$), and (b) reversible metal cation expulsion upon electrochemical oxidation to the dicationic state. A channel-like solid-state structure is observed for the Ba^{2+} complex ($C_{20}H_{30}O_5S_8$, $Ba^{2+}(CF_3SO_3)_2^{2-}$, $(H_2O)_2$, CD_3CN, monoclinic $C2/c$, $Z = 8$, $a = 45.66(1)$ Å, $b = 8.897(5)$ Å, $c = 23.124(8)$ Å, $\beta = 105.54(4)°$, $V = 9050$ Å^3), which results from the segregated stacking mode of the crown ether and the redox-active tetrathiafulvalene subunits, respectively.

Introduction

It is now well established that the attachment of a crown ether to a redox-active unit, such as a metallocene or quinone, affords a macrocycle in which the metal cation complexing ability of the ligand can be tuned according to the electrochemical potential applied.[1]

Owing to its three reversible oxidation states, the tetrathiafulvalene (TTF) unit has recently emerged as an alternative electroactive system in the design of redox responsive ligands which are able to recognize cationic guests electrochemically.[2] Indeed, TTF derivatives present three redox stages (neutral, radical cation, and dication), and therefore they possibly allow not only binding but also electrochemical releasing of metallic cations to be achieved. Nevertheless, none of the crown ether TTF derivatives described so far fully satisfy the requisite criteria for a truly efficient redox-active metal cation sponge. Indeed, either they display a low metal binding ability together with poor electrochemical discrimination of their complexing properties[3] or the synthetic strategies used so far have led to severely bent systems, resulting in a breakdown of the classical well-defined electrochemical behavior of the parent TTF unit.[4,5]

In this context, we have designed the ligand system **1** which fulfills all the required prerequisites to act as a very efficient Ba^{2+} redox responsive ligand, which notably exhibits an unprecedented high coordination ability among tetrathiafulvalene-based macrocycles when the redox moiety is neutral, and furthermore which allows complete cation expulsion when dicationic.

Since the largest HOMO coefficients of the isolated TTF core are known to be located on the central $S_2C{=}CS_2$ fragment,[6]

* To whom correspondence should be addressed. Phone: +33 (0)2 41 73 54 39. Fax: +33 (0)2 41 73 54 05. E-mail: marc.salle@univ-angers.fr (M.S.).
† UMR CNRS 6501, Université d'Angers.
‡ SC RMN, Université d'Angers.
§ Odense University.
⊥ CSIC-Universidad de Zaragoza.
⊗ Université d'Oran Es-Senia.

(1) For reviews related to this topic, see for instance: (a) Boulas, P. L.; Gómez-Kaifer, M.; Echegoyen, L. *Angew. Chem., Int. Ed. Engl.* **1998**, *37*, 216. (b) Kaifer, A. E.; Mendoza, S. In *Comprehensive Supramolecular Chemistry, Vol. 1*; Atwood, J. L., Davies, J. E., MacNicol, D. D., Vögtle, F., Eds.; Pergamon: Oxford, 1996; pp 701−732. (c) Beer, P. D.; Gale, P. A.; Chen, G. Z. *Coord. Chem. Rev.* **1999**, *185−186*, 3.

(2) (a) Le Derf, F.; Mazari, M.; Mercier, N.; Levillain, E.; Richomme, P.; Becher, J.; Garín, J.; Orduna, J.; Gorgues, A.; Sallé, M. *Chem. Commun.* **1999**, 1417. (b) Le Derf, F.; Sallé, M.; Mercier, N.; Becher, J.; Richomme, P.; Gorgues, A.; Orduna, J.; Garin, J. *Eur. J. Org. Chem.* **1998**, 1861. (c) Brøndsted, M.; Becher, J. *Liebigs Ann.* **1997**, 2177 and references therein. (d) Jørgensen, T.; Hansen, T. K.; Becher, J. *Chem. Soc. Rev.* **1994**, 41 and references therein.

(3) (a) Hansen, T. K.; Jørgensen, T.; Stein, P. C.; Becher, J. *J. Org. Chem.* **1992**, *57*, 6403. (b) Dieing, R.; Morisson, V.; Moore, A. J.; Goldenberg, L. M.; Bryce, M. R.; Raoul, J. M.; Petty, M. C.; Garin, J.; Saviron, M.; Lednev, I. K.; Hester, R. E.; Moore, J. N. *J. Chem. Soc., Perkin Trans. 2* **1996**, 1587.

(4) Hansen, T. K.; Jørgensen, T.; Jensen, F.; Thygesen, P. H.; Christiansen, K.; Hursthouse, M. B.; Harman, M. E.; Malik, M. A.; Girmay, B.; Underhill, A. E.; Begtrup, M.; Kilburn, J. D.; Belmore, K.; Roespstorff, P.; Becher, J. *J. Org. Chem.* **1993**, *58*, 1359.

(5) Wang, C.; Bryce, M. R.; Batsanov, A. S.; Howard, J. K. *Chem. Eur. J.* **1997**, *3*, 1679 and references therein.

(6) Lowe, J. P. *J. Am. Chem. Soc.* **1980**, *102*, 1262.

10.1021/ic9907617 CCC: $18.00
Published on Web 12/03/1999

Table 1. Crystallographic Data for (*Z*)-**1** and (*Z*)-**1**−$Ba(CF_3SO_3)_2$·CD_3CN·$2H_2O$

	(*Z*)-**1**	(*Z*)-**1**−$Ba(CF_3SO_3)_2$·CD_3CN·$2H_2O$
empirical formula	$C_{20}H_{30}O_5S_8$	$C_{24}H_{37}NO_{13}F_6S_{10}Ba$
fw	606.97	1119.53
space group/*Z*	$P\bar{1}/2$	$C2/c/8$
temp (K)	293	293
a (Å)	9.087(6)	45.66(1)
b (Å)	11.637(7)	8.897(5)
c (Å)	14.370(8)	23.124(8)
α (deg)	65.54(3)	90
β (deg)	82.32(5)	105.54(4)
γ (deg)	84.18(6)	90
volume (Å^3)	1368 (1)	9050(10)
radiation (Mo Kα)	$\lambda = 0.710\ 73$ Å	$\lambda = 0.710\ 73$ Å
ρ_{calcd} (g·cm^{-3})	1.47	1.64
no. of independent reflns ($I > 3\sigma(I)$)/no. of variables	1665/298	2062/301
R/R_w (F_ϕ)[a]	0.056/0.077	0.103/0.118

[a] $R = \sum(|F_\phi| - |Z_k|F_\phi|)/\sum|F_\phi|$, $R_w = \sum w^{1/2}(|F_\phi| - |Z_k|F_\phi|)/\sum w^{1/2}|F_\phi|$.

the crown subunit in **1** has been introduced along the long axis of the redox-active TTF core (i.e., on the 2,7-positions of the TTF unit), instead of vicinal 2,3-positions, resulting in a structural arrangement which optimizes the interaction between the guest cation and the electroactive TTF core. Furthermore, the size of the lateral polyether chain in **1** has been chosen large enough to avoid any severe bending of the TTF framework and to allow a suitable cavity size for cation binding.

Experimental Section

^{1}H and ^{13}C NMR spectra were recorded on a Bruker Advance DRX500 operating at 500 and 125.7 MHz, respectively. δ are given in parts per million (relative to TMS) and *J* values in hertz. ^{1}H NMR titration experiments were carried out as follows (constant temperature, 22 °C): seven NMR tubes were each filled with 15.0 mg of compound **1** and the adequate amount of $Ba(CF_3SO_3)_2$ (i.e., 0, 0.25, 0.5, 0.75, 1, 2, and 5 equiv, respectively), the total volume being adjusted to 1 mL with a $CD_3CN/CDCl_3$ (1:1, v/v) solution ([**1**] = 0.0248 mol·L^{-1}). This solvent mixture proved to be the best compromise to solubilize both constituents (compound **1** and $Ba(CF_3SO_3)_2$). Mass spectra were recorded on a VG-Autospec (Micromass, U.K.). EI mass spectra were obtained at 70 eV, and accurate mass measurements were performed at 10 000 resolution (peak width at 5% height) using PFK as internal reference. LSI mass spectra were obtained using the standard Cs^+ gun operated at 30 kV. For the determination of absolute binding constants, the spectra of NBA solutions (2 μL) containing **1** (0.05 M) and variable $Ba(ClO_4)_2$ concentrations were recorded. Electrochemical experiments were carried out with a PAR 273 potentiostat−galvanostat in a three-electrode single-compartment cell equipped with platinum microelectrodes of 7.85×10^{-3} cm^2 area, a platinum wire counter electrode, and a Ag/AgCl reference electrode. Cyclic voltammetry was performed in methylene chloride/acetonitrile (1:1, v/v) solutions (SDS, HPLC grade) containing 0.10 M tetrabutylammonium hexafluorophosphate (TBAHP) (Fluka puriss). Solutions were deaerated by argon bubbling prior to each experiment which was run under inert atmosphere.

X-ray Structural Analyses and Structure Refinements. (*Z*)-**1**: $C_{20}H_{30}O_5S_8$, red prismatic crystal ($0.7 \times 0.2 \times 0.2$ mm^3), $\mu = 0.655$ mm^{-1}, 2−23° θ range, $0 \le h \le 9$, $-12 \le k \le 12$, $-15 \le l \le 15$, 3727 independent reflections measured (1665 reflections with $I/\sigma(I) > 3$) (Table 1). (*Z*)-**1**−$Ba(CF_3SO_3)_2$·CD_3CN·$2H_2O$: brown prismatic crystals ($0.4 \times 0.3 \times 0.2$ mm^3), $\mu = 1.395$ mm^{-1}, $T_{min} = 0.55 - T_{max} = 1$, 2−21° θ range, $-45 \le h \le 45$, $0 \le k \le 8$, $0 \le l \le 23$, 5354 independent reflections measured (2062 reflections with $I/\sigma(I) > 3$) (Table 1).

For both crystals, X-ray diffraction data were collected at 293 K on an Enraf Nonius MACH3 four-circle diffractometer ($\lambda_{Mo\ K\alpha} = 0.710\ 69$) equipped with a graphite monochromator. All calculations were performed using the MolEN package (Lorentz-polarization, absorption corrections (difabs), direct methods, refinements). For (*Z*)-**1**−$Ba(CF_3SO_3)_2$·CD_3CN·$2H_2O$, the poor quality of the data (2062 reflections available) did not allow the structure resolution to be brought to a successful conclusion, especially for most atoms belonging to the crown ether part and to $CF_3SO_3^-$ entities, since a disorder phenomenon probably affects these atoms. As a consequence, thermal motion of several atoms appears significantly larger, and O (five atoms from eight), N, F, and C atoms were refined isotropically. Finally, refinements of 301 parameters from 2062 reflections converged to $R = 0.103$.

Scheme 1

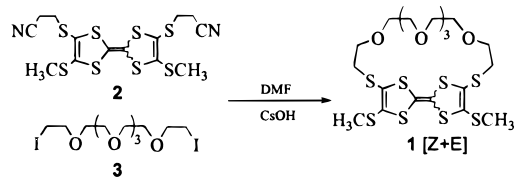

Synthetic Procedure. [*E*,*Z*]-3,6(7)-Bis(methylsulfanyl)-2,7(6)-(4,7,10,13,16-pentanoxa-1,19-dithianonadecane-1,19-diyl)tetrathiafulvalene (1). A methanolic solution (10 mL) of cesium hydroxide (0.37 g, 2.2 mmol) is added at room temperature under nitrogen to a stirred solution of compound **2**[7] (0.466 g, 1 mmol) in dry DMF (50 mL). After 15 min of stirring, the resulting mixture and a solution of 1,17-diiodo-3,6,9,12,15-pentaoxaheptadecane (**3**) in 60 mL of DMF are both transferred under nitrogen into two syringes connected to a perfusor pump. Both solutions are then simultaneously added very slowly (5 mL/h) under nitrogen at room temperature into a round-bottom flask containing 200 mL of DMF. When addition is complete (12 h), the mixture is allowed to stir for an additional 3 h. Solvents are then evaporated in vacuo. The oil obtained is dissolved in methylene chloride (50 mL), washed with water (3 × 50 mL), and dried over sodium sulfate. After evaporation, the residue is chromatographed on a silica gel column (methylene chloride/ethyl acetate, 9:1). Evaporation of solvents and precipitation in methanol afford pure **1** as a bright orange solid (0.33 g, 55%). Slow diffusion of pentane vapors to compound **1** dissolved in methylene chloride afford single crystals of [*Z*]-**1** prone to X-ray diffraction. Single crystals of [*Z*]-**1**-$Ba(CF_3SO_3)_2$·CD_3CN·$2H_2O$ suitable for X-ray analysis are obtained by slow diffusion of pentane vapors to the previous $CD_3CN/CDCl_3$ ^{1}H NMR titration solutions. [*Z*]-**1**/[*E*]-**1** = 9 (^{1}H NMR). [*Z*]-**1**: ^{1}H NMR ($CDCl_3$, 500 MHz) δ 3.58 (s, 20H, CH_2O), 2.93 (t, 4H, SCH_2), 2.40 (s, 6H, SCH_3); ^{13}C NMR ($CDCl_3$, 125.7 MHz) δ 131.6, 125.8, 112.2, 71.9, 71.85, 71.8, 71.7, 71.2, 36.3, 20.2. [*E*]-**1**: ^{1}H NMR ($CDCl_3$, 500 MHz) δ 3.65−3.54 (m, 20H, CH_2O), 2.91 (m, 4H, SCH_2), 2.41 (s, 6H, SCH_3); ^{13}C NMR ($CDCl_3$, 125.7 MHz) δ 132.4, 126.2, 112.5, 72.0, 71.73, 71.72, 71.71, 71.7, 36.5, 20.2. $C_{20}H_{30}O_5S_8$: MS (EI):$M^{\bullet+}$ (calcd) 605.9859; $M^{\bullet+}$ (found) 605.9840. Anal. (calcd): C, (39.60) 39.27; H, (4.99) 4.87; O, (13.25) 13.54; S, (42.21) 42.60.

Results and Discussion

Receptor **1** was prepared (55%), under high dilution conditions in DMF, from the [1+1] cyclocondensation of compound **2**[7] with *ω*-diiodopentaethylene glycol (**3**),[8] in the presence of cesium hydroxide (Scheme 1), and was obtained as a *Z*/*E* isomeric mixture in relative amounts of 90:10, as determined by ^{1}H NMR.

The molecular structure of the (*Z*)-**1** isomer was confirmed by X-ray crystallography (Figure 1 and Table 1). As expected, the degree of bending in the TTF skeleton is very low. Indeed, distortion from planarity of the TTF subunit, defined as the angle between the line C(1)═C(2) on one hand and the plane incorporating S(1)S(2)C(4)C(3) (or S(3)S(4)C(6)C(5)) on the other hand, is as low as 5.1° in (*Z*)-**1**. This corresponds to a

(7) Becher, J.; Lau, J.; Leriche, P.; Mørk, P.; Svenstrup, N. *J. Chem. Soc., Chem. Commun*. **1994**, 2715.
(8) (a) Dale, J.; Kristiansen, P. O. *Acta Chem. Scand*. **1971**, *26*, 1471. (b) Li, H. M.; Post, B; Morawetz, H. *Makromol. Chem*. **1972**, *154*, 89.

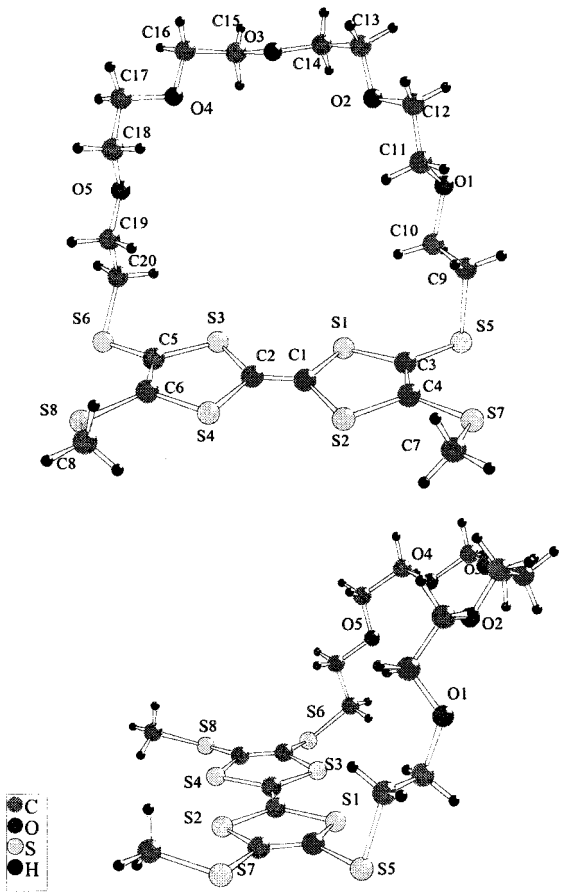

Figure 1. Molecular structure of (*Z*)-**1** in the solid state.

significant improvement in the degree of planarity as compared with the value of 34.5° observed with previous fused crown ether TTF derivatives.[4,9] This structural feature is of crucial importance, since the TTF backbone is known to lose its well-defined reversible electrochemical properties—and therefore applicability in redox responsive ligands—when bending becomes significant, as observed with previously described crown ether TTF systems.[4]

Apart from an important contribution toward the planarity of the TTF unit, the use of a long polyether chain also ensures a suitable cavity size for the inclusion of a guest cation, and furthermore allows the coordinating oxygen atoms to orientate toward the center of the cavity in (*Z*)-**1** (Figure 1), a structural environment highly suited for the incorporation of a metal cation.

Complexation Studies. Mass spectrometry has proved to be a powerful tool in the study of host−guest chemistry.[10] Thus, the capability of FABMS to reproduce crown ether selectivity toward metal cations was reported[10b] soon after the introduction of this technique. However, competitive binding studies in which a ligand is mixed with a molar equivalent of each of a series of cations have been reevaluated,[10c] and it has been concluded that the ionization efficiency of each metal−ligand complex is strongly influenced by the nature of the matrix. Hence, this means of determining binding selectivity is invalid unless the ionization efficiencies are also estimated. The study of the influence of the matrix on the stability constants measured by LSIMS led to the conclusion that hydrophobic matrixes such as *m*-nitrobenzyl alcohol (*m*-NBA) limit the influence of solvation on the desorption of the dissolved ionic species,[10d] and the authors proposed a method of determining the stability constants that involves the previous determination of ionization efficiencies in terms of desorption coefficients.[10e]

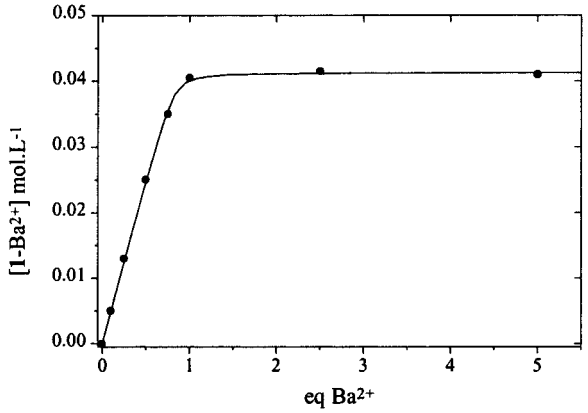

Figure 2. LSI MS (NBA matrix) titration curve of compound **1** on addition of barium cation ($Ba(ClO_4)_2$).

A different picture is obtained when absolute binding constants are studied since the classic method proposed by Bonas and co-workers[10f] determines the desorption coefficients relating peak intensities to metal−ligand complex concentrations, thus considering the effect of the matrix on the ionization process and yielding binding constants that are in reasonable agreement with those determined by other means in solvents having dielectric constants similar to those of the used matrixes.

The Ba^{2+} binding constant of **1** was evaluated by LSIMS (positive ionization mode) in *m*-NBA as the matrix. The method[2b,10f] involved the experimental measurement of the peak intensity of the host−guest complex with progressive increasing of the metal concentration (the $[2M + H]^+$ peak of the matrix at *m*/*z* 307 was used as internal standard). The stability constant was given by a curve-fitting program which calculated the best fit between theoretical and experimental concentrations.

Host **1** has a marked affinity for Ba^{2+} over other metal cations of group 1 or 2 with formation of a 1:1 complex observed by LSI mass spectrometry (*m*/*z* 843, (*Z*)-**1**−$Ba(ClO_4)^+$; *m*-NBA). It is noteworthy that the addition of an excess of Ba^{2+} resulted in complexation of only 90% of the total crown ether **1**. This result, along with the 90/10 *Z*/*E* ratio of compound **1** determined from NMR experiments, confirms that Ba^{2+} is trapped by the *Z* isomer only. Calculation[10f] of the binding constant from LSIMS titration study (Figure 2) gave a $K°$ value of $10^{3.49}(\pm 3 \times 10^2)$ (*m*-NBA matrix).

An NMR titration experiment was carried out in $CDCl_3$/CD_3CN (1:1), using ligand **1** and barium trifluoromethanesulfonate. The crown ether methylene protons of (*Z*)-**1** (δ = 3.57 ppm) are shifted to a lower field upon addition of Ba^{2+}, which confirms that complexation to the polyether subunit is taking place. Moreover, the resulting titration curve (Figure 3) exhibits a plateau for 1 equiv of added cation relative to (*Z*)-**1**.

(9) A trans-substitution by a $S(CH_2)_{12}S$ bridge allowed the TTF skeleton to be essentially planar: Boubekeur, K.; Lenoir, C.; Batail, P.; Carlier, R.; Tallec, A.; Le Paillard, M. P.; Lorcy, D.; Robert, A. *Angew. Chem., Int. Ed. Engl.* **1994**, *33*, 1379.

(10) (a) For a review see: Vincenti, M. *J. Mass Spectrom.* **1995**, *30*, 925. b) Johnstone, R. A. W.; Rose, M. E. *J. Chem. Soc., Chem. Commun.* **1983**, 1268. (c) Langley, G. J.; Hamilton, D. G.; Grossel, M. C. *J. Chem. Soc., Perkin Trans. 2* **1995**, 929. (d) Giraud, D.; Scherrens, I.; Lever, M. L.; Laprévote, O.; Das, B. C. *J. Chem. Soc., Perkin Trans. 2* **1996**, 901. (e) Giraud, D.; Laprévote, O.; Das, B. C. *Org. Mass Spectrom*. **1994**, *29*, 169. (f) Bonas, G.; Bosso, C.; Vignon, M. R. *Rapid Commun. Mass Spectrom*. **1988**, *2*, 88.

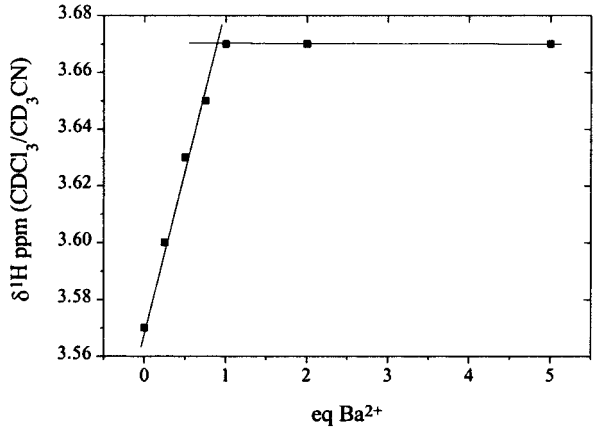

Figure 3. Proton NMR titration curve of the perturbation of the $-CH_2O-$ protons of the polyether bridge in **1** on addition of barium cation ($Ba(CF_3SO_3)_2$).

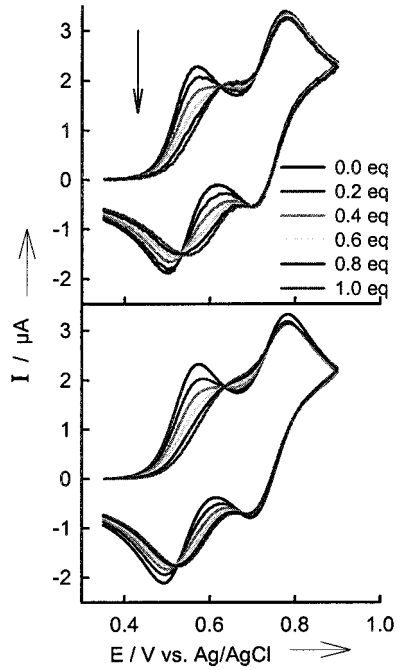

Figure 4. Experimental (top) and simulated (bottom) cyclic voltammograms of compound **1** in the presence of increasing amounts of Ba^{2+}. The simulated data were fitted to experimental results for **1** (10^{-3} mol·L^{-1} in CH_2Cl_2/CH_3CN (1:1), Bu_4NPF_6 (0.1 mol·L^{-1}), at 293 K and 100 mV s^{-1}) according to Scheme 2. All simulations were carried out with the same set of parameters, except the Ba^{2+} equivalent concentration was changed according to the experimental voltammograms. Charge-transfer parameters: $k_s = 0.01$ cm s^{-1}, $\alpha = 0.5$. Chemical reaction parameters: $K° = 1.6 \times 10^4$ mol^{-1} L, $k_f° = 2 \times 10^6$ mol^{-1} L s^{-1}, and $K^{\bullet+} = 2.4\ 10^2$ mol^{-1} L, $k_f^{\bullet+} = 1.5 \times 10^3$ mol^{-1} L s^{-1}. Diffusion coefficient $D = 1.35 \times 10^{-5}$ cm^2 s^{-1}.

Analysis of these data with the program EQNMR[11] shows that the crown ether recognition site of (*Z*)-**1** forms a 1:1 complex with Ba^{2+}, with a stability constant value of $K° = 10^{4.17} \pm 10^3$.

The recognition properties of the redox-active receptor **1** were also evaluated by cyclic voltammetry (CH_2Cl_2/CH_3CN, 1:1). Contrary to observations made on previous fused crown ether TTF derivatives and, as expected from the quasi-planar structure discussed above, compound **1** exhibits two reversible one-electron redox processes ($E_1^{ox} = 0.53$ V and $E_2^{ox} = 0.73$ V vs Ag/AgCl) (Figure 4).

Scheme 2

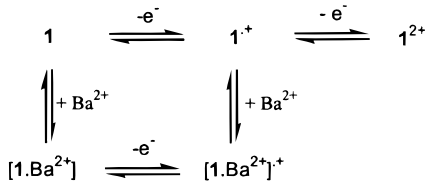

Another remarkable, albeit expected, feature of ligand **1** is the effect of the Ba^{2+} complexation on its electrochemical behavior. A significant change in the cyclic voltammogram of **1** could be observed during the addition of Ba^{2+} to the electrolytic solution. The progressive addition of controlled amounts of barium perchlorate to cage TTF **1** (as a CH_2Cl_2/CH_3CN (1:1) solution, Bu_4NPF_6 (0.1 mol·L^{-1})) led to a substantial anodic shift of the first oxidation potential (E_1^{ox}) (Figure 4). Noteworthy, this behavior was not manifested when alternative group 1 or 2 or transition metal ions were used (Li^I, Na^I, Rb^I, Cs^I, Mg^{II}, Ca^{II}, Sr^{II}, Cr^{III}, Ni^{II}, Cd^{II}),[12] which is a good indication of the selectivity of ligand **1** for Ba^{2+}. On the other hand, E_2^{ox} of ligand **1** remained unchanged upon addition of Ba^{2+}. The anodic shift of E_1^{ox} observed with increasing [Ba^{2+}] is believed to arise from an electrostatic inductive effect of the crown ether bound metal cation, which results in a decrease of electron density in the TTF moiety. On the other hand, the fact that the E_2^{ox} value is not altered upon addition of Ba^{2+} could be attributable to the expulsion of the positive metal ion from the cavity, due to the increased repulsive electrostatic interaction with the doubly charged TTF moiety.

Interestingly, the E_1^{ox} shift determined by cyclic and square wave voltammetry reaches a limit ($\Delta E = 100$ mV) for a stoichiometric amount of added metal. This constitutes a striking improvement compared to crown ether TTF derivatives described so far, for which more than a 250 excess of added metal cation was necessary to achieve a saturation of the system.[3]

The efficiency in modulation of the trapping properties of the redox responsive ligand **1** was evaluated using the DIGISIM 2.1 simulation program (BAS Inc.)[13] (Figure 4 and Scheme 2). In accordance with the expected electrochemical control of the complexation/expulsion process, the binding constant of the Ba^{2+} complex depends on the oxidation state of the redox-active TTF core: (a) a very strong affinity is found for the neutral TTF state ($K° = 10^{4.28}(\pm 2.2 \times 10^3)$); noteworthy, this value is in excellent agreement with the one determined by NMR ($K° = 10^{4.17}$ ($CDCl_3/CD_3CN$ (1:1)); (b) a striking decrease of the complexation ability is observed for $TTF^{\bullet+}$ ($K^{\bullet+} = 10^{2.38} \pm 29$); (c) finally a $K^{2+} \approx 0$ value is found for the dicationic TTF^{2+} state, which could be attributable to the expulsion of the metal, as shown by the constant E_2^{ox} value.

Therefore, contrary to previous claims which state the metal cation expulsion to occur at the radical cation stage,[3a] calculations made on the basis of the equilibria of Scheme 2 show a partial expulsion for $TTF^{\bullet+}$, and a complete one for the TTF^{2+} state, in accordance with the increased repulsive electrostatic interaction occurring at the doubly charged state. Therefore, TTF derivative **1** appears to be a very attractive redox system, compared for instance to the extensively studied ferrocene-based ligands, for which the monocharged oxidized form cannot allow full control of the metal cation expulsion process.

(11) Hynes, M. J. *J. Chem. Soc., Dalton Trans.* **1993**, 311.

(12) Addition of $Cu(CF_3SO_3)_2$ or $Hg(CF_3CO_2)_2$ to **1** in CH_2Cl_2/CH_3CN led to oxidation of the ligand.

(13) Rudolph, M.; Reddy, D. P.; Feldberg, S. W. *Anal. Chem.* **1994**, *66*, 589A.

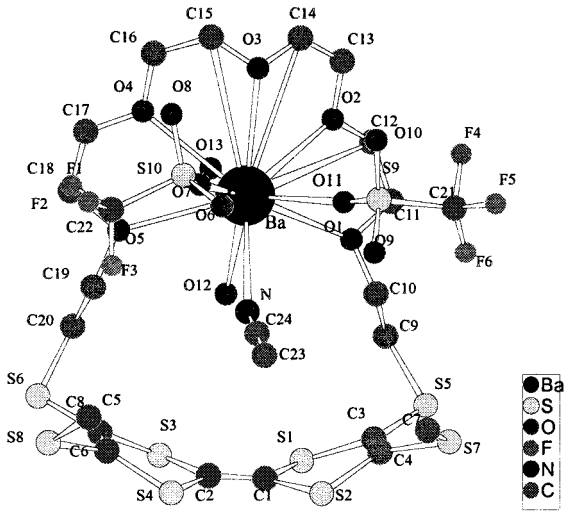

Figure 5. Molecular structure of [(*Z*)-**1**−$Ba(CF_3SO_3)_2$·CD_3CN·$2H_2O$] in the solid state.

Finally, the slow diffusion of pentane vapors to the previous NMR titration solutions afforded medium-quality crystals of the corresponding complex.

The X-ray crystal structure of [(*Z*)-**1**−$Ba(CF_3SO_3)_2$·CD_3CN·$2H_2O$] is shown in Figure 5. Analysis of the molecular structure shows that the metal atom is located in the center of the cavity and is 10-fold coordinated by the five oxygen atoms of the polyether subunit (Ba···O 2.88(5)−2.92(3) Å), four oxygen atoms of two triflate anions and two water molecules (Ba···O 2.72(3)−2.87(4) Å), and one nitrogen atom of an acetonitrile molecule (Ba···N 2.99(5) Å). Insertion of the barium cation in the cavity induces an important conformational perturbation of receptor (*Z*)-**1**: the bending angle of the TTF skeleton changes from 5.1° in the free ligand to 29.6° in the complex.

The packing mode of this system is of striking interest since the TTF core and the polyether fragment are stacked in a segregated way, giving rise to molecular channels where the metallic cations are located (Figure 6). This unique pattern of overlap leads to a two-dimensional association, where slabs of the complexing polyether subunits are separated by the electroactive ones.

In conclusion, the efficiency of compound **1** as a redox responsive ligand has been demonstrated by (a) an unprecedented metal cation binding ability among crown ether TTF derivatives (neutral TTF state), including the first X-ray structural determination of a metal complex based crown ether TTF, and (b) the first evidence of controllable expulsion of the metal cation from the cavity, upon electrochemical oxidation to the dicationic TTF state.[14]

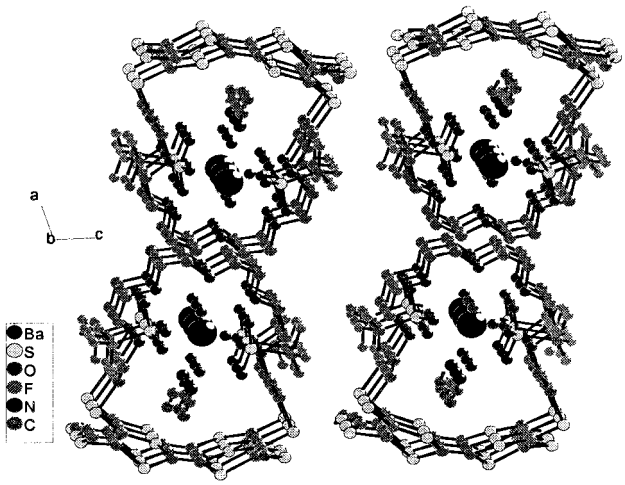

Figure 6. Stacking mode of [(*Z*)-**1**−$Ba(CF_3SO_3)_2$·CD_3CN·$2H_2O$].

Furthermore, the channel-like solid-state structure of a metal-coordinated crown−TTF system opens a wide range of exciting challenges, notably in the field of electron and ion transports in stacked systems[15] as well as in the interrelation between electrical (TTF redox site) and magnetic properties, e.g., by coordination of a transition metal possessing unpaired spins.[16]

Supporting Information Available: ^{1}H NMR spectrum of compound **1** (*Z*/*E* = 90/10), square wave voltammograms (SWV) of compound **1** in the presence of increasing amounts of Ba^{2+}, and two X-ray crystallographic files ([*Z*]-**1** and [*Z*]-**1**−$Ba(CF_3SO_3)_2$·CD_3CN·$2H_2O$), in CIF format. This material is available free of charge via the Internet at http://pubs.acs.org.

Acknowledgment. Financial support from CNRS, MESR, and DGICYT (Grant PB97-1186 and Action Intégrée HF1997-0042) is gratefully acknowledged.

IC9907617

(14) For analogous observations with metallocene-based redox-active ligands, see: Plenio, H.; Burth, D. *Organometallics* **1996**, *15*, 1151.
(15) Sielcken, O. E.; Van de Kuil, L. A.; Drenth, W.; Schoonman, J.; M. Nolte, R. J. *J Am. Chem. Soc.* **1990**, *112*, 3086.
(16) (a) Coronado, E.; Gomez-Garcia, C. J. *Chem. Rev.* **1998**, *98*, 273. (b) Kurmoo, M.; Graham, A. W.; Day, P.; Coles, S. J.; Hursthouse, M. B.; Caulfield, J. L.; Singleton, J.; Pratt, F. L.; Hayes, W.; Ducasse, L.; Guionneau, P. *J Am. Chem. Soc.* **1995**, *117*, 12209. (c) Gomez-Garcia, C. J.; Ouahab, L.; Gimenez-Saiz, C.; Triki, S.; Coronado, E.; Delhaes, P. *Angew. Chem., Int. Ed. Engl.* **1994**, *33*, 223.